# FUNCTIONAL CHARACTERISTICS OF RECONSTITUTED SARCOPLASMIC RETICULUM MEMBRANES AS A FUNCTION OF THE LIPID-TO-PROTEIN RATIO

L. HERBETTE, A. SCARPA, and J. K. BLASIE, *Departments of Chemistry and Biochemistry/Biophysics, University of Pennsylvania, Philadelphia, Pennsylvania 19104*

D. R. BAUER, *Engineering and Research Division, Ford Motor Company, Dearborn, Michigan 48421*

C. T. WANG AND S. FLEISCHER, *Department of Molecular Biology, Vanderbilt University, Nashville, Tennessee 37235*

ABSTRACT The ATP-induced $Ca^{2+}$ accumulation efficiency and rates of $Ca^{2+}$ uptake of the reconstituted sarcoplasmic reticulum (RSR) model membrane system were measured over an extended range of lipid-to-protein (L/P) molar ratios and were compared to those of isolated light sarcoplasmic reticulum (LSR). Highly purified sarcoplasmic reticulum (SR), dissociated in the presence of deoxycholate, was reconstituted for several L/P ratios, according to the same procedure, forming closed membraneous vesicles composed of >95% $Ca^{2+}$ pump protein and SR lipids which were capable of ATP-induced $Ca^{2+}$ accumulation in the absence of oxalate or other $Ca^{2+}$ precipitating agents. This suggests that dissociation of SR and reconstitution to form RSR does not significantly affect the ability of the $Ca^{2+}$ pump protein incorporated into the SR lipid bilayer to establish $Ca^{2+}$ gradients. Electron micrographs of fixed and stained dispersions of RSR revealed a structural organization of the membrane that was dependent upon the L/P molar ratio. RSR with L/P >88 were composed of closed vesicles whose membranes stained asymmetrically, similar to that observed for LSR. Closed vesicles of RSR with L/P <88 were composed of membranes that stained symmetrically. In addition, reconstituted SR preparations with well-defined L/P molar ratios >88 possess a functional behavior similar to that of LSR (in the absence of oxalate, energy efficiencies are 60–70% and apparent initial uptake rates are 80% that of isolated LSR controls); RSR preparations with L/P <88 are characterized by significantly depressed values of the energy efficiencies and apparent initial uptake rates especially at low L/P ratios. Thus, we are the first to report a reconstituted SR model membrane system capable of attaining rates of $Ca^{2+}$ uptake comparable to isolated LSR controls at comparable L/P ratios in the absence of oxalate or other $Ca^{2+}$ precipitating agents.

## INTRODUCTION

The dissociation of a membrane into its lipid and protein components and the reconstitution of a functional membrane complex from these pure components can help determine the relationship between the structure and function of membranes. The sarcoplasmic reticulum membrane is particularly appropriate for such studies, owing to its relatively simplified function and composition (1–5). The regulatory role in the contraction-relaxation cycle of the sarcoplasmic reticulum membrane has been associated with the control of the concentration

of $Ca^{2+}$ in the sarcoplasm (6, 7). Most of our knowledge on the mechanism of active ion transport in the sarcoplasmic reticulum membrane system has been obtained through the use of fragmented sarcoplasmic reticulum isolated in the form of closed membraneous vesicles that retain a permeability barrier against $Ca^{2+}$, and which, being energized with an ATP-$Mg^{2+}$ substrate, are known to accumulate $Ca^{2+}$ against a large concentration gradient (2, 5, 8).

The sarcoplasmic reticulum membrane consists of 40% phospholipid and 60% protein. Most of the phospholipid is lecithin (73%), which is present along with two other major lipids, phosphatidylethanolamine (14%) and phosphatidylinositol (9%). In highly purified sarcoplasmic reticulum (SR)[1] three proteins predominate (9, 10), with the $Ca^{2+}$ pump protein the major component (75%). Highly purified SR can be subfractionated to provide "light" (LSR) and "heavy" (HSR) sarcoplasmic reticulum, which differ in that the latter contains electron opaque material which has been shown to be mainly the $Ca^{2+}$ binding protein (11). In both, the main component of the membrane is the $Ca^{2+}$ pump protein comprising >95% of the total protein. The molecular weight of the $Ca^{2+}$ pump protein has been shown to be 102,000 (12, 13), or, more recently, 119,000 (14). We use the latter value to calculate the lipid-to-protein (L/P) molar ratios. The fact that hydrated oriented multilayers of SR and LSR vesicles can give rise to extensive meridional lamellar x-ray and neutron diffraction (15–17), coupled with simplicity of function and composition, makes the SR membrane system and its reconstituted membrane systems particularly suited for a structure-function correlation study.

Functional as well as structural characteristics of the isolated SR membrane have been investigated by several authors (15, 16, 18). Such studies are obviously limited by the fact that the molar ratio of lipid and protein in the membrane of isolated SR vesicles is necessarily constant. Dissociation and reassembly of the SR membrane into functional membraneous vesicles has been achieved (19). Furthermore, methodology has now been developed to prepare reconstituted sarcoplasmic reticulum membrane vesicles (RSR) of varying L/P ratio in a range suitable for the study of lipid-protein interactions, i.e., both higher and lower lipid content as compared with the original SR membrane (20); this overcomes the limitations intrinsic to the isolated SR membrane. Hence, membrane reconstitution and functional studies in conjunction with structural studies utilizing x-ray and neutron diffraction can be used to investigate the manner in which systematic structural perturbations affect the function of the membrane.

In this paper, we report estimates of the initial rates of $Ca^{2+}$ uptake and the $Ca^{2+}$/ATP energy efficiency ratios for RSR vesicles over an extended range of L/P ratios. The steady-state accumulation levels were obtained and corrected for the effective internal vesicular volume. We have also determined the dependence of the $Ca^{2+}$ loading efficiency (i.e., mole of $Ca^{2+}$ uptake per mole of ATP hydrolyzed as based on the phosphoenzyme formation of SR for which 2 mol $Ca^{2+}$ and 1 mol $P_i$ are bound per mole of $Ca^{2+}$ pump protein [21, 22]) of the RSR vesicles in the presence of oxalate over this range of L/P ratios. We report the first simultaneous monitoring of ATP-induced $Ca^{2+}$ uptake and ATPase activity in SR vesicular dispersions using a spectrophotometric technique (16, 23).

[1]In this paper SR will refer only to the highly purified sarcoplasmic reticulum prepared according to Meissner et al. (24); specifically, light, intermediate, and heavy sarcoplasmic reticulum, designated LSR, ISR, HSR, respectively, will refer to the upper, intermediate and lower fractions obtained from the isopycnic gradient (11).

## METHODS

### *Dissociation of SR and Reconstitution of RSR*

SR were isolated from rabbit skeletal muscle, purified by zonal centrifugation and suspended in a solution containing 300 mM sucrose, 100 mM KCl, 1 mM Hepes, pH 7.1 (24). The suspension of purified SR vesicles obtained in this manner was solubilized in 400 mM sucrose, 450 mM KCl, 1 mM EDTA, 1.5 mM $MgCl_2$, 0.1 mM $CaCl_2$, 10 mM Tris-HCl (pH 7.9) in the presence of deoxycholate. Reconstitution of this solubilized fraction into membraneous RSR vesicles with different L/P ratios was achieved by adding various amounts of purified SR lipid before dialysis (20). RSR vesicles were checked for homogeneity by inspection of the sedimentation pattern after centrifugation on a sucrose gradient. RSR samples were washed several times with dialysis buffer, suspended in 300 mM sucrose, 100 mM KCl, and 1 mM Hepes at pH 7.1, quickly frozen in liquid nitrogen, and stored at −70°C until use. Protein concentrations of the samples were determined by the method of Lowry et al. (25), using bovine serum albumin as a standard; phospholipid phosphorus was estimated from the total phosphorus (9), which was measured by the Fiske-Subbarow method (30). The L/P ratio calculated from these measurements is expressed as mole phospholipid per mole protein (mole PL/mole prot) throughout this paper.

### *Electron Microscopy of RSR Dispersions*

Dispersions of RSR at several different L/P ratios along with isolated LSR were fixed by the tannic acid-$OsO_4$ method previously described (26). Thin sections were cut on an LKB Ultratome (LKB Instruments, Inc., Rockville, Md.) with diamond knives (E. I. DuPont de Nemours and Co., Wilmington, Del.), and subsequently examined in a Hitachi HU-11b electron microscope (Tokyo, Japan).

### *Functional Assays of SR and RSR Vesicles*[2]

$Ca^{2+}$ UPTAKE[2] AND ATPASE ACTIVITY $Ca^{2+}$ uptake and ATPase activity were measured simultaneously by a dual wavelength spectrophotometric technique using arsenazo III as a metallochromic indicator of ionized $Ca^{2+}$ and phenol red as an indicator of free $H^+$ concentrations. Under defined conditions, changes in ionized $Ca^{2+}$ concentrations produce linear increments in the absorbance ($\Delta A$) of arsenazo III (23). Likewise, changes in the $H^+$ concentration produce linear increments in the absorbance of phenol red. The simultaneous changes in absorbance of each dye present in the reaction mixture were measured with a time-sharing multichannel spectrophotometer (23). At the wavelength pair ($\lambda_1$-$\lambda_2$) of 675–685 nm, ionized $Ca^{2+}$ concentration changes can be measured selectively with arsenazo III. Likewise, at the wavelength pair ($\lambda_3$-$\lambda_4$) of 507–540 nm, changes in the concentration of $H^+$ produced by the cleavage of ATP can be selectively measured without interference from $Ca^{2+}$ transients. Nonspecific absorbance changes due to changes in volume and/or refractive indices of the vesicles were minimized or abolished by the time-sharing measurement at two wavelengths in close proximity.

Assays of RSR and SR were monitored as dispersions (1 mg/ml) in 2 ml final volume containing 100 mM KCl, 10 mM $MgCl_2$, 2 mM Tris maleate (medium I), with 50 $\mu$M arsenazo III and/or 50 $\mu$M phenol red at pH 7.0. Separate and simultaneous measurements of the $Ca^{2+}$ uptake and ATPase activities were recorded and were found to be similar. The kinetics of the $Ca^{2+}$ uptake reaction, along with the generation of $H^+$ due to ATP hydrolysis, were continuously monitored for several minutes following the addition of ATP. In these experiments A23187 or X537A, two ionophores which equilibrate $Ca^{2+}$ transients across SR vesicles (27), were added in the steady state upon near depletion of ATP. Calibrations of the absorbance changes of arsenazo and phenol red were obtained by adding

[2]We will use the terms "$Ca^{2+}$ loading" and "$Ca^{2+}$ uptake" to refer to energized $Ca^{2+}$ accumulation or pumping measured in the presence and absence, respectively, of a $Ca^{2+}$ precipitating agent such as oxalate (19). For each term we can refer to a rate, a capacity, and an efficiency of $Ca^{2+}$ pumping. The latter term is defined as the number of moles of $Ca^{2+}$ pumped per mole of ATP hydrolyzed.

known concentrations of $CaCl_2$ and NaOH, respectively, to the reaction mixture. For dispersions of SR at the pH of the reaction (pH 7.1), approximately 1.0 mol of protons were produced per mole of ATP cleaved as determined by $OH^-$ titrations of the reaction. Our values were similar to those obtained by Alberty et al. (28) and Yamada et al. (29), where 0.8–0.9 mol of protons were generated per mole of ATP split in a medium similar to ours in both composition and pH. For RSR dispersions, the final pH of the reaction mixture was usually 6.8, following addition of RSR to medium I at pH 7.0. Under these conditions, 0.5 mole protons were produced per mole of ATP cleaved.

Alternatively, ATPase activity of SR dispersions (1 mg/ml) was measured in 2 ml of suspension medium at 22°C and pH 7.0 in the absence of dye indicators. After the addition of 150–300 $\mu$M of ATP, aliquots of the reaction mixture were taken at 15, 30, 60 and 120 s, added to 0.5 ml 10% trichloroacetic acid, and assayed for inorganic phosphate by the method of Fiske and Subbarow (30), as modified by Chen et al. (31). These amounts of inorganic phosphate formed from ATP hydrolysis were compared to those determined before addition of ATP.

### *$Ca^{2+}$ Loading and ATPase Activity in the Presence of Oxalate*

$Ca^{2+}$ loading and ATPase activity of RSR in the presence of oxalate, which forms a precipitate of calcium oxalate inside the vesicles, were measured under similar conditions, as previously described (19, 20). The amount of $Ca^{2+}$ taken up by RSR vesicles in the first 1 min interval, i.e., where the reaction kinetics are linear with time, represents the $Ca^{2+}$ loading rate expressed as $\mu$mol $Ca^{2+}$ /mg · min. The $Ca^{2+}$ loading efficiency is thus the ratio of this loading rate and the $Ca^{2+}$-stimulated ATPase activity rate ($\mu$mol $P_i$/mg · min).

### *Measurement of SR and RSR Intravesicular Volume*

The intravesicular water spaces of SR, RSR, HSR, and LSR vesicles were measured by a radiochemical technique. $^3H_2O$ and either [$^{14}$C]polydextran (70,000–90,000 mol wt), [$^{14}$C]polydextran (20,000 mol wt), or [$^{14}$C]Inulin (5,000–5,500 mol wt) were added to centrifuge tubes containing variable amounts of SR vesicles (0.5–1.5 mg) suspended in medium I at pH 7.0. After 15 min incubation at room temperature the samples were centrifuged at 20,000 rpm for 90 min in a Beckman SW 27 swinging bucket rotor (Beckman Instruments Inc., Spinco Div., Palo Alto, Calif.). Aliquots of the supernatant fluid (1 or 5 $\mu$l) were added to 0.2 ml of perchloric acid (50%), along with 0.1 ml of suspension medium. The pellets were gently washed twice in suspension medium and carefully blotted dry before being placed in 0.1 ml of suspension medium and sonicated for several minutes to disperse the packed pellets. To this dispersion 0.2 ml of perchloric acid (50%) were added and samples were incubated for more than 48 h at room temperature. All samples were subsequently centrifuged at 3,200 rpm for 15 min and 0.1 ml of the supernatant fluid was added to 5 ml of Handiflour scintillation fluid (Mallinckrodt, Inc., St. Louis, Mo.) containing 0.2 ml of 3 M formic acid and counted for $^3$H and $^{14}$C radioactivity. The internal water space was calculated as the difference of the total water space and the excluded polydextran space of the pellet.

Control experiments involved separately centrifuging the $^{14}$C isotopes in 0.4 ml of suspension medium, in the absence of SR containing $^3H_20$ for 90 min at various $g$ values (10,000–100,000 $g$). Aliquots of 1 or 5 $\mu$l were carefully sampled from the top, middle, and bottom portions of each tube. The results of these experiments are shown in Fig. 1, where the ratios of the counts per minute (cpm) for aliquots sampled at the bottom relative to the top are plotted as a function of the $g$-force for each of the $^{14}$C isotopes. The distribution of each of the $^{14}$C isotopes was uniform throughout the top and middle portions of the centrifuge tube (not shown), increasing only at the bottom of each tube by the relative amounts indicated in Fig. 1. The actual distributions of the $^{14}$C isotopes presented here are specific to the composition and pH of the suspension medium that was used in our experiments. Other buffer systems may yield somewhat different results. Appreciable binding of the $^{14}$C isotopes to the SR vesicles was excluded, based on control experiments carried out with SR as previously described for isolated chromaffin granules (32). Thus, the excluded volumes were calculated and corrected for the appropriate $^{14}$C distributions and subtracted from the total $^3H_20$ space to yield the intravesicular water content. In light of these experimental results, we feel that re-evaluation of the intravesicular volumes of other

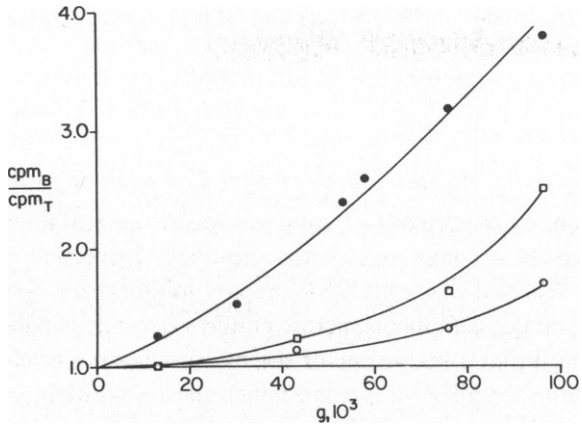


FIGURE 1 Distribution of $^{14}C$ isotopes at the bottom relative to the top of centrifugation cells as a function of the centrifugal *g*-force. The *g*-force dependence is seen to be most significant for [$^{14}C$]polydextran (70,000–90,000 mol wt) (●), as compared with [$^{14}C$]polydextran (20,000 mol wt) (□), and [$^{14}C$]Inulin (5,000–5,500 mol wt) (○). Suspension medium (minus SR) contained $^3H_2O$ in addition to either of the $^{14}C$ isotopes and was used as an internal control ($^3H_2O$ was distributed uniformly throughout the centrifugation cell as expected). $cpm_B/cpm_T$ refers to the ratio of the counts per minute in a comparable aliquot at the bottom and top of the tube, respectively.

membraneous vesicle systems determined by this or similar procedures should be carried out, owing to the fact that the excluded volumes calculated on the basis of the $^{14}C$ content of the supernatant fluid with respect to that trapped in the pellet may be artifactually high, thus yielding lower internal volumes based on the dependence of the $^{14}C$ distribution on the centrifugal *g*-force (33–36).

### *Measurement of RSR Vesicle Size via Quasielastic Light Scattering*

A 5 mW Spectra-Physics He-Ne laser operating at 632.8 nm was used as the light source. The incident light was focused on a 1-cm square quartz cell containing RSR (0.05 mg/ml) in medium I, pH 7.0. The buffer was filtered through 0.2 N Gelman GA metrecel filters (Gelman Sciences, Inc., Ann Arbor, Mich.) to remove dust before RSR preparations were added, with all measurements made at room temperature (25 ± 1°C). Scattered light was detected with a RCA C31034A photomultiplier (RCA Electro-Optics & Devices, Lancaster, Pa.) in a cooled (−20°C) housing. The photocurrent was amplified and then frequency analyzed with a Saicor-51B spectrum analyzer (Honeywell, Hauppauge, N.Y.). Spectra with a signal-to-noise ratio of 50:1 could be obtained in a few minutes. The power spectrum of light scattered from a monodisperse sample has a Lorentzian line shape whose halfwidth at half height is given by $2\mathbf{q}^2D$, where $\vec{\mathbf{q}}$ is the scattering vector and $D$ is the translational diffusion coefficient (37). These spectra were plotted with an *XY* recorder and the halfwidths were determined graphically. Diameters were calculated from the measured diffusion coefficient and the Stokes-Einstein equation, utilizing data obtained at scattering angles of 22°, 40.5°, and 90°.

### *Materials*

Na-ATP and arsenazo III were purchased from Sigma Chemical Co. (St. Louis, Mo.). Arsenazo III was passed through columns of Chelex 100 obtained from Bio-Rad laboratories (Richmond, Calif.) to remove $Ca^{2+}$ contamination. Phenol Red ($Na^+$ salt) was a product of J. T. Baker Chemical Co. (Phillipsburg, N.J.). A23187 and X537A were kindly provided by Dr. Hamill of Eli Lilly and Co. (Indianapolis, Ind.) and from Dr. Burger of Hoffman-LaRoche (Nutley, N. J.), respectively. Deoxycholate (Matheson, Coleman, and Bell, Norwood, Ohio) was recrystallized before use (24). [$^{14}C$]polydextran (2.763 mCi/g, 20,000 mol wt), [$^{14}C$]polydextran (1.043 mCi/g, 70,000 – 90,000 mol wt),

[$^{14}$C]Inulin (2.110 mCi/g, 5,000 – 5,500 mol wt) and $^{3}H_2O$ (1.0 mCi/g) were purchased from New England Nuclear (Boston, Mass.).

## RESULTS

### *Homogeneity and Uniformity in Membrane Composition of RSR Preparations*

Each RSR preparation of a particular L/P ratio was washed several times with dialysis buffer and separately placed on a continuous sucrose gradient. Inspection of the sedimentation pattern in every case revealed that each RSR preparation formed a single tight band whose position (i.e., density) on this continuous sucrose gradient depended upon the L/P ratio of that particular preparation. From a knowledge of the measured width of each band (which was approximately the same for all RSR preparations) and its position, one can calculate the density distribution and hence the L/P ratio distribution for each preparation. Such a calculation has revealed that the statistical spread in the L/P ratios for each RSR preparation we report in this and the following paper is small, being on the order of ±1%.

The L/P ratios for each individual RSR preparation were directly measured by separate determinations of the total phosphorus and total protein. Total phosphorus was used as an estimate of lipid phosphorus, since phospholipid headgroups represent the only source of phosphorus. The protein composition of all RSR preparations, as determined by SDS gel-electrophoresis, was found to be >95% $Ca^{2+}$ pump protein. Hence, these L/P ratio determinations may be expressed as the number of moles of phospholipid to the number of moles of $Ca^{2+}$ pump protein. Protein and phosphorus determinations were obtained several times for each RSR preparation, yielding an overall statistical error in our *measured* L/P molar ratio determinations on the order of ±2%, comparable to the *calculated* statistical spread in L/P ratios determined by density gradient centrifugation.

### *Electron Microscopy of Fixed Dispersions of RSR*

Dispersions of RSR were stained and fixed according to the methods described (26), revealing important features of these RSR preparations. Fig. 2 shows the results of the tannic acid-$0s0_4$ fixation method for isolated LSR (*A*), RSR with L/P equal to 92.8 (*B*) and 45.2 (*C*). It is immediately evident that both isolated and reconstituted SR preparations are composed of *closed* membraneous vesicles. In fact, all RSR preparations with different L/P ratios (data not shown) have this essential characteristic. In addition to this, inspection of these micrographs reveals the uniformity in membrane composition for the two different RSR preparations shown. This negates the possibility that some vesicles contain more or less significant amounts of protein compared with the average and is in agreement with the sucrose density centrifugation results described above. However, the packing density of the protein was found to depend on the L/P ratio especially for L/P>88 (data not shown). Inspection of several micrographs taken from a broad field for each different RSR preparation confirmed these results. Details of the localization of heavy staining for each preparation are given in the legend to Fig. 2. This Figure is representative of RSR preparations with L/P<88 and L/P>88. Thus, our preparations are homogeneous and uniform in composition, being composed of closed membraneous vesicles whose functional properties are described below.

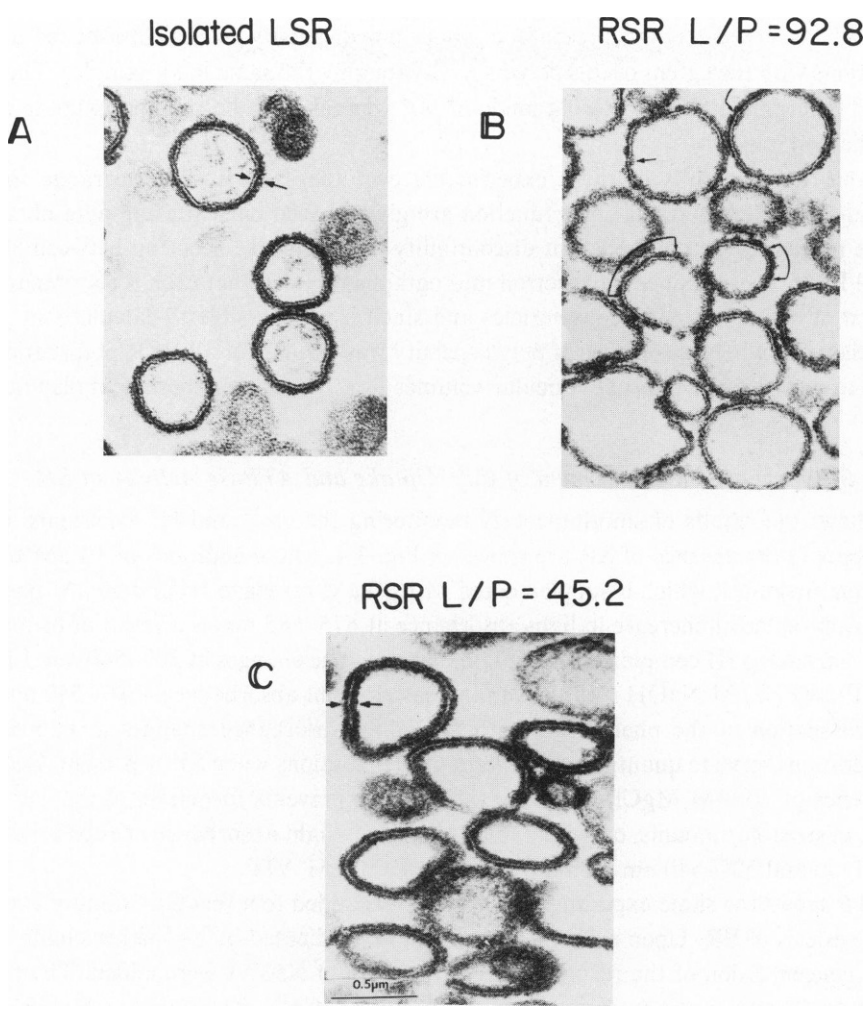


FIGURE 2 *A* An electron micrograph of membraneous vesicles of isolated LSR fixed via the tannic acid-osmium method. The arrows indicate the localization of heavy staining exclusively in the extravesicular half of the LSR membrane for those regions of the membrane profiles in the plane of thin sectioning. Similar experiments were carried out with RSR, L/P equal to 92.8 and 45.2, shown in *B* and *C*, respectively. In *B* the bracketed arrows indicate the predominant localization of heavy staining in the extravesicular half of the RSR membrane, as observed in LSR, with the occasional appearance of heavy staining in the intravesicular half of the membrane for those regions of the membrane profiles in the plane of thin sectioning. This is true for all RSR preparations with L/P > 88. In *C* heavy staining occurs equally in both halves of the RSR membrane. This is true for all RSR preparations with L/P < 88. (We note that the heavy metal-staining images of vesicular dispersions of RSR shown in Saito et al. (26) were all for preparations with L/P < 88).

### *Vesicle Size of RSR as a Function of the L/P Ratio*

We have carried out a preliminary investigation of the RSR vesicle size vs. L/P ratio via quasi-elastic light scattering (38). A frequency analysis of the noise spectra of the light scattering from RSR samples allowed a determination of the diffusion coefficient from which the vesicle diameter was calculated. Spectra obtained at various scattering angles of 22°,

40.5°, and 90° indicated the presence of some polydispersity in vesicle size for all RSR preparations with the extent of this polydispersity roughly the same in all samples. The vesicle diameter determined at a scattering angle of 90° was taken to be the approximate average vesicle diameter.

In Table I, the results of these experiments over the same L/P ratio range for RSR investigated in characterizing their function are given, based on scattering data obtained at 90°. The results suggest an apparent discontinuity in vesicle size occuring between 88.4 and 96.8 mol PL/mol prot. Since the electron micrographs revealed that each RSR preparation is composed of closed membraneous vesicles and since it was possible to calculate an average vesicle diameter where the degree of polydispersity was similar for all RSR preparations, it is possible to measure the internal vesicular volumes as a function of the L/P molar ratio (see Fig. 5).

### *Simultaneous Measurement of $Ca^{2+}$ Uptake and ATPase Activity of SR*

Fig. 3 shows the results of simultaneously monitoring the $Ca^{2+}$ and $H^+$ transients. Control experiments in the absence of SR are shown in Fig. 3*A*, where additions of 10 $\mu$M $CaCl_2$ to suspension medium I, which is supplemented with 50 $\mu$M arsenazo III and 50 $\mu$M phenol red at pH 7.0, produce an increase in light absorbance at 675–685 nm as a result of formation of the $Ca^{2+}$ -arsenazo III complex with negligible absorbance changes at 507–540 nm. Likewise, the addition of 50 $\mu$M NaOH results in an increase in light absorbance at 507–540 nm due to the deprotonation of the phenol red, with negligible absorbance changes at 675–685 nm. These additions serve to quantitate the extent of the reactions when SR is present. Because of the presence of 10 mM $MgCl_2$ in the medium, which prevents formation of the $Ca^{2+}$ -ATP complex in sizeable amounts, only very small changes in light absorbance are observed at both 675–685 nm and 507–540 nm with the addition of 150 $\mu$M ATP.

Fig. 3*B* shows the same experiments when ATP is added to a reaction mixture containing isolated vesicles of SR. Upon exhaustion of the ATP (indicated by no further changes in the free $H^+$ concentration of the reaction medium), 20 $\mu$g of X537A were added. The resulting absorbance changes are consistent with ATP-induced $Ca^{2+}$ accumulation by SR and its release upon addition of the $Ca^{2+}$ ionophore. In parallel experiments, under identical conditions, ATP hydrolysis was also followed by the time-course of inorganic phosphate formation, as measured by the method of Chen et al. (31). These values of ATP hydrolysis are plotted in Fig. 3*B* (open circles), and are very similar to those obtained by phenol red measurements. Appearance of inorganic phosphate is thus seen to be quantitatively consistent with proton formation, as measured by phenol red, thus verifying the spectrophotometric

TABLE I
RSR VESICLE DIAMETER VS. L/P RATIO VIA QUASIELASTIC LIGHT SCATTERING

| L/P | Diameter | L/P | Diameter |
|---|---|---|---|
| *(mol PL/mol prot)* | *(Å)* | *(mol PL/mol prot)* | *(Å)* |
| 55.3 | 1,790 | 96.5 | 2,730 |
| 66.5 | 1,550 | 106.1 | 2,580 |
| 81.1 | 1,510 | 126.8 | 2,680 |
| 87.3 | 1,680 | 142.9 | 2,240 |

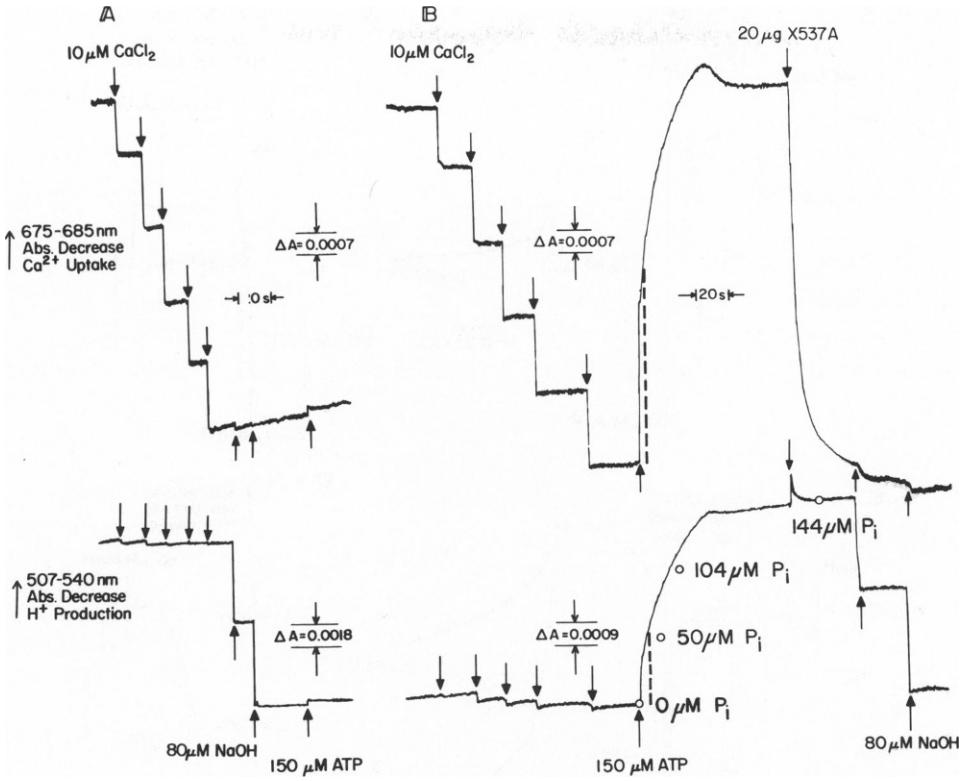


FIGURE 3 *A*, Simultaneous changes in light absorbance undergone by arsenazo III and phenol red upon addition of $CaCl_2$, ATP, and NaOH to the reaction mixture in the absence of SR. *B*, Simultaneous measurements of ATP-induced $Ca^{2+}$ accumulation and ATPase activity of SR vesicles. The reaction mixtures contained medium I supplemented with 50 μM arsenazo III, 50 μM phenol red, and SR (1 mg protein/ml). Owing to the difficulty in adjusting the pH of an ATP-$Mg^{2+}$ solution, free ATP ($Na^+$ form) was used and adjusted to pH 7.8. Formation of the ATP-$Mg^{2+}$ complex when ATP is added to the reaction medium results in changes of the $pK_a$ at 6.8 of ATP, so that one must adjust the pH of the ATP solution to ~ 0.8 pH units more basic than that of the reaction medium in these low capacity buffer systems in order to ensure a negligible change in pH of the final reaction mixture upon the addition of ATP. The open circles coincident with the ATPase trace in *B* represent the time-course of inorganic phosphate production. The dotted vertical line on each trace represents the initial 5-s interval of the reaction.

approach described above. The $Ca^{2+}/P_i$ ratio measured at the 5-s interval (dotted line in Fig. 3*B*) for SR under these experimental conditions is ~ 0.5.

### *$Ca^{2+}$ Uptake and ATPase Activity of RSR*

Fig. 4 shows the results of several experiments where the ATP-dependent $Ca^{2+}$ uptake by RSR and LSR vesicles in dispersion was monitored by the arsenazo III method along with separate measurements of the ATPase activity by the phenol red method. In Fig. 4*A*, the addition of 300 μM ATP to a reaction mixture containing RSR (1 mg/ml) with a L/P ratio of 60.0 mole PL/mol prot results in ATP-induced $Ca^{2+}$ transport by RSR. With the attainment of the steady state [under these conditions] in 50–60 s, an accumulation of 40 nmol $Ca^{2+}$/mg prot was calculated. The addition of 30 μg of X537A causes the release of the accumulated $Ca^{2+}$. In this and subsequent figures showing the reaction kinetics of $Ca^{2+}$ uptake, identical

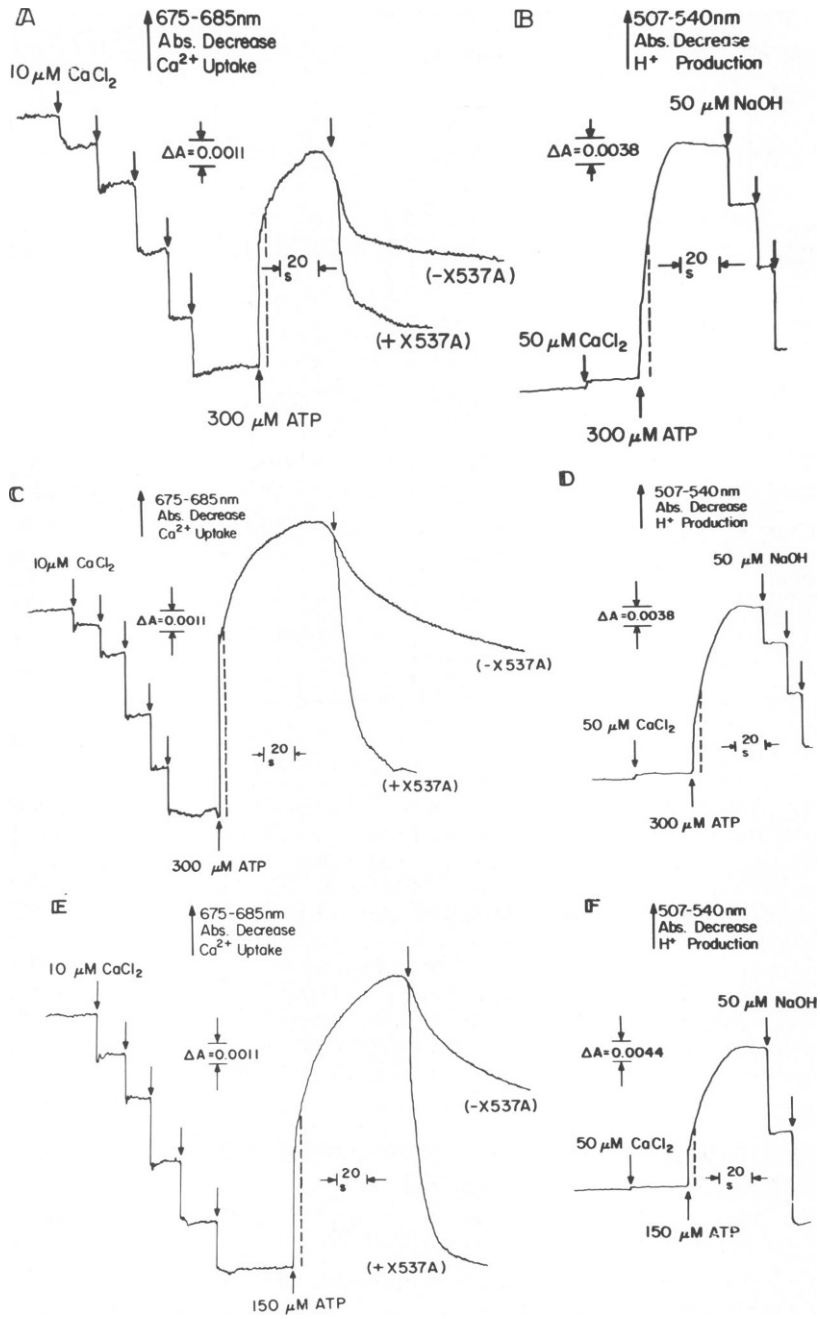


FIGURE 4 Measurement of $Ca^{2+}$ uptake and ATP hydrolysis by RSR. *A*, ATP-induced $Ca^{2+}$ uptake by RSR with a L/P ratio equal to 60.0 mol PL/mole prot. *B*, ATPase activity of the same RSR preparation measured under identical conditions. *C* and *D*, Analogous assays for RSR with a L/P ratio equal to 122.7 mole PL/mole prot. *E* and *F*, Control assays with isolated LSR (L/P equal to 115.3 mol PL/mol prot) measured under similar conditions. Reaction mixture contained medium I, either RSR (1 mg prot/ml) or LSR (0.5 mg prot/ml), and 50 μM arsenazo III (*A*, *C*, *E*), or 50 μM phenol red (*B*, *D*, *F*). All reactions were carried out at 23°C. The dotted vertical line on each trace represents the initial 5-s interval of the reaction.

experiments with and without the addition of ionophore are superimposed. In Fig. 4*B*, RSR (1 mg/ml) with the same L/P ratio as in Fig. 4*A* is present in a reaction mixture supplemented with 50 $\mu$M phenol red at pH 7.0, but otherwise identical to that in Fig. 4*A*. When ATP is added, a production of protons commences, which is consistent with ATP hydrolysis, until a plateau is reached, indicating the depletion of all the ATP. Similar results with RSR for a L/P ratio of 122.7 mol PL/mol prot are shown in Figs. 4*C* and *D*, for comparison. The steady-state accumulation was calculated to be 70 nmol $Ca^{2+}$/mg prot. Control assays were carried out using LSR (0.5 mg/ml), since we feel that LSR most closely reflects the function and composition of the RSR system (Figs. 4*E*, *F*). Owing to the higher efficiency of isolated LSR, it was necessary to carry out this assay under conditions where both the ATP and LSR concentrations were one-half of what they were for assaying RSR preparations. Thus LSR vesicles accumulated 110 nmol $Ca^{2+}$/mg prot.

These results indicate that RSR preparations, especially for those with a L/P ratio in the range of 38.5 – 84.0 mol PL/mol prot possess a relatively high rate of ATP hydrolysis. Also it is interesting to note that LSR and RSR with comparable L/P ratios have similar passive leak kinetics, as followed spectrophotometrically for several minutes subsequent to the depletion of ATP under conditions where both RSR and LSR have accumulated similar amounts of $Ca^{2+}$ (see Fig. 3 *C*, *E* and Discussion).

### *Intravesicular Volume of RSR as a Function of the L/P Ratio*

The measurement of the intravesicular volume for the various RSR preparations was found to depend upon the L/P molar ratio. Owing to the fact that the protein content of RSR prepared as described above is mainly $Ca^{2+}$ pump protein (>95%), the intravesicular water space thus obtained is one important variable which should affect the ultimate steady-state accumulation of $Ca^{2+}$. As shown in Fig. 5, the intravesicular volume expressed as $\mu$l $H_2O$/mg prot, determined by the radioisotope methods described above, is plotted as a function of the L/P ratio and is found to have a bell-shaped dependence on the protein content per vesicle. These

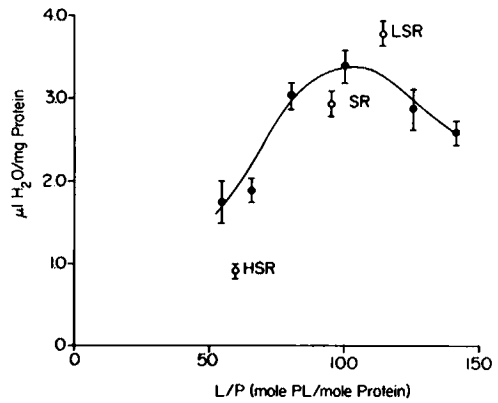


FIGURE 5 Intravesicular water space vs. the L/P ratio of RSR (●), LSR, SR, HSR via the $^3H_2O$ and [$^{14}$C]polydextran method. The ratio of the counts in the supernatant fluid and pellet yielded the total water space ($^3H_2O$) and the excluded space [$^{14}$C]polydextran). Their difference corresponds to the intravesicular water space, which is plotted here. The bars on each data point represent the experimental error determined from several assays and a smooth curve was drawn through the average.

data are consistent with the vesicle diameters shown in Table I; especially note at higher L/P both vesicle diameter and volume begin to fall. This additional experimental result can be used to express the steady-state accumulation data as nmol $Ca^{2+}/\mu l$ internal water. The steady-state levels for $Ca^{2+}$ uptake of all RSR preparations could be as high as 85% when compared with LSR controls. (This value was similar for *all* RSR preparations, being equal to 23 nmol $Ca^{2+}/\mu l$ water compared to 27 for LSR). In addition, the variation in the intravesicular space over the L/P range investigated is one factor which could account for the variability in time required for attaining the $Ca^{2+}$ uptake steady state of the various RSR preparations.

### *Apparent Initial Rates of $Ca^{2+}$ Uptake and $Ca^{2+}$ Pumping Efficiency ($Ca^{2+}$/ATP) of RSR as a Function of the L/P Ratio*

In order to gain information regarding the efficiency of the RSR membrane system compared with isolated LSR, it is essential to determine the dependence of the initial rates of $Ca^{2+}$ uptake vs. L/P ratio. From kinetic curves similar to those shown in Figs. 3 and 4, estimates to the initial rates of $Ca^{2+}$ uptake were calculated over the first several seconds of the reaction and expressed as nmol $Ca^{2+}$/mg prot · 5 s. We realize that these "initial" rates represent at most an approximation to the true initial rates, owing to the fact that the reaction proceeds linearly only over the first 400–800 ms in the case of isolated SR, as determined by Inesi and Scarpa (39) using a fast-flow technique. However, owing to the fact that large amounts of RSR material not presently available are required for stop-flow measurements, we emphasize the need to determine approximately the initial $Ca^{2+}$ uptake event in the first 5-s interval in the absence of oxalate. Thus, as shown by the dotted line in Fig. 4, the $Ca^{2+}$ uptake attained in the first 5 s of the reaction can easily be determined directly from the traces. For times <5s, significant errors may be introduced into the calculation. Fig. 6*A* shows the results of such experiments where the log of the initial rates is plotted vs. L/P ratio. The log of the $Ca^{2+}$ pumping efficiency was also considered as a function of the L/P ratio, as shown in Fig. 6*B*. By definition the $Ca^{2+}$ pumping efficiency is the ratio of $Ca^{2+}$ accumulated in the initial part of the reaction, i.e., where $Ca^{2+}$ uptake proceeds linearly, to the ATP hydrolyzed during this same time period. Owing to the variability in the $Ca^{2+}$ uptake efficiency for different RSR preparations, we have presented the results of several experiments from several preparations over the indicated L/P range. For RSR with L/P >88 the estimated initial rates as we have defined them were all similar, equal to 35 nmol $Ca^{2+}$/mg prot 5 s, and the $Ca^{2+}$ uptake efficiencies of the best preparations were 0.26 nmol $Ca^{2+}$/nmol ATP. For the sake of comparison, the estimated initial rate and the $Ca^{2+}$ uptake efficiency were determined for LSR under similar conditions and found to be 45 nmol $Ca^{2+}$/mg prot 5 s and 0.61 nmol $Ca^{2+}$/nmol ATP, respectively. Owing to the variability of initial rate data inherent in isolated membrane preparations, it is possible at this stage of our investigation only to point out that these estimated initial rates of $Ca^{2+}$ uptake of RSR preparations with L/P ratios similar to that of LSR are comparable to that of LSR. At lower L/P ratios, especially around 50–60, RSR preparations are seen to function significantly poorer compared with LSR.

### *$Ca^{2+}$ Loading and ATPase Rates of RSR in the Presence of Oxalate*

The results in Fig. 4 showed that RSR vesicles are capable of ATP-induced $Ca^{2+}$ uptake when assayed as the dispersion in the absence of oxalate. In Fig. 7*A* the $Ca^{2+}$ loading rate (in the

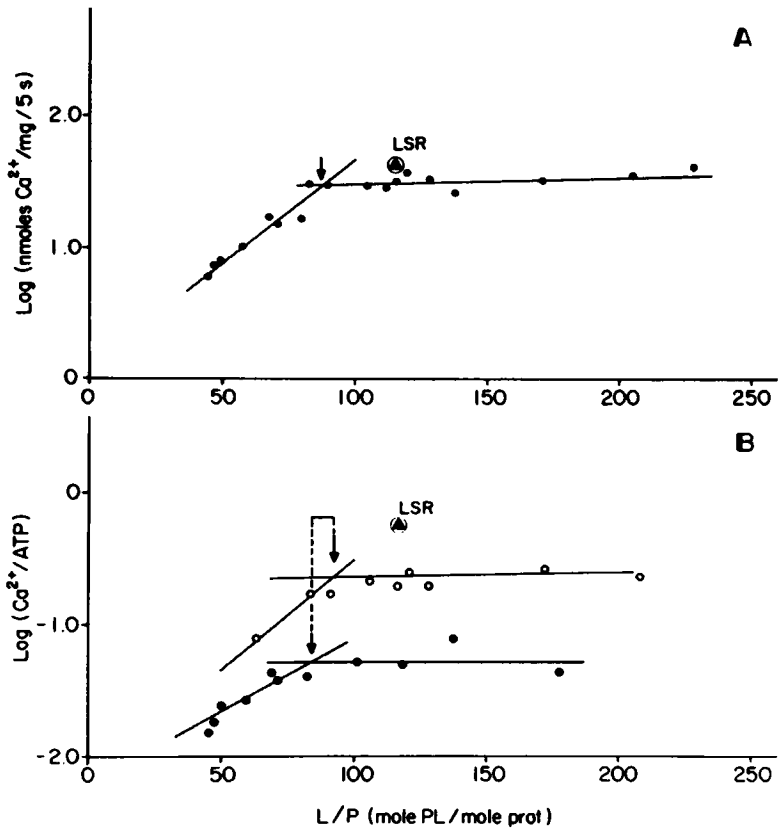


FIGURE 6 Measurement of the $Ca^{2+}$ uptake initial rates and efficiencies of RSR in the absence of oxalate as a function of the L/P ratio. *A*, Log plots of the estimated initial rates of $Ca^{2+}$ uptake (averaged over the first 5 s of the reaction) as a function of the L/P ratio. The data are expressed here as nmol $Ca^{2+}$/mg · 5 s, and represent the accumulation before saturation occurs. This curve is a composite of several different RSR preparations. *B*, $Ca^{2+}$ uptake efficiency vs. L/P ratio. The log of the $Ca^{2+}$ uptake efficiency is calculated from the log of the initial $Ca^{2+}$ uptake rate divided by the total ATPase rate averaged over the first 5 s of the reaction. The different curves show the variability in $Ca^{2+}$ uptake efficiency for different RSR preparations (○, ●) over their indicated L/P range. The efficiencies reported here are calculated using the *total* ATPase activity. If the $Ca^{2+}$-stimulated ATPase rates were used, the efficiencies would be higher than they appear in *B* (See Discussion).

presence of oxalate) and the ATPase rate are plotted vs. the L/P ratio for dispersions of RSR assayed in the presence of 5 mM oxalate. The $Ca^{2+}$ loading rate is seen to be a monotonically decreasing function of the L/P ratio. Oxalate forms a precipitate with $Ca^{2+}$ inside the RSR vesicles, thereby effectively decreasing the intravesicular $Ca^{2+}$ concentrations of these membraneous vesicles. Likewise, in Fig. 7*A*, the ATPase rate measured under similar conditions was plotted vs. the L/P ratio, yielding a monotonically increasing dependence on L/P ratio. Thus, the $Ca^{2+}$ loading efficiency, the ratio of the $Ca^{2+}$ loading rate to the ATPase rate ($\mu$M $Ca^{2+}$/$\mu$M $P_i$), is found to increase monotonically as the protein content of the RSR vesicle increases, as shown in Fig. 7*B*. The measurements of $Ca^{2+}$ loading and ATPase rates along with the efficiency ratio in the presence of oxalate for the LSR preparation whose L/P ratio is usually ~ 116.7 mol PL/mol prot are 5.8 $\mu$mol $Ca^{2+}$/mg · min, 2.6 $\mu$mol $P_i$/mg · min,

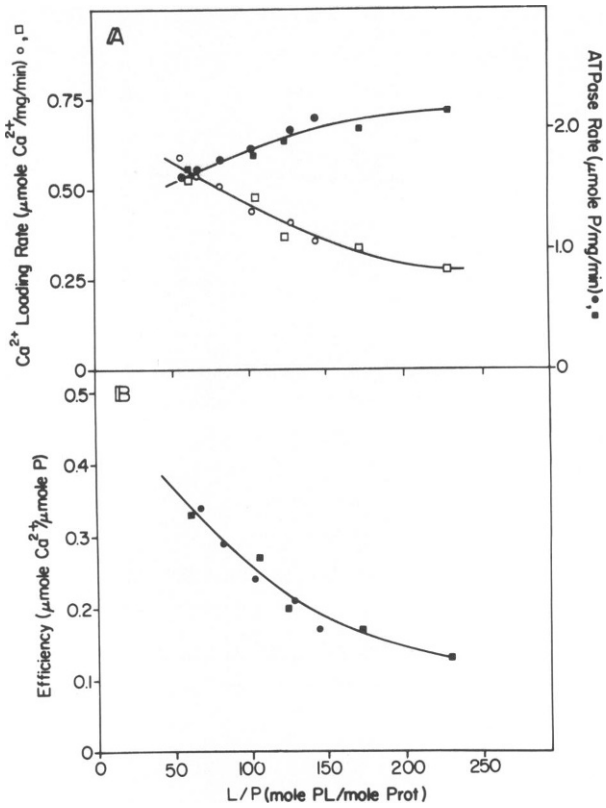


FIGURE 7 Measurement of the $Ca^{2+}$ loading rate, ATPase rate, and $Ca^{2+}$ loading efficiency (i.e., as measured in the presence of oxalate) of RSR as a function of the L/P ratio. *A*, $Ca^{2+}$ loading rate (○, □) and ATPase rate (●, ■) of RSR as a function of the L/P ratio. (○, ●) represent the results from one RSR preparation; whereas (□, ■) refer to another RSR preparation. *B*, $Ca^{2+}$ loading efficiency, i.e., ratio of the $Ca^{2+}$ loading rate to the ATPase rate ($\mu M$ $Ca^{2+}/\mu M$ $P_i$) of RSR as a function of the L/P ratio. The efficiencies were calculated from the data of the two preparations shown in *A*, with (●) referring to the first preparation and (■) to the second. In *A* and *B* the reaction mixture contained 100 mM KCl, 5 mM $MgCl_2$, 10 mM Hepes, pH 7.0, 5 mM oxalate, and RSR (5–20 $\mu$g prot/ml), along with 5 mM ATP and 100 $\mu M$ $^{45}Ca^{2+}$. Reactions were carried out at 23°C.

and 2.2 $\mu$mol $Ca^{2+}/\mu$mol $P_i$, respectively. The individual assays are normalized to one another, since they are based on equal amounts of protein, usually ~ 20 $\mu$g/assay.

## DISCUSSION

### *Comparison with Other Reconstituted SR Membrane Systems*

Reconstitution techniques offer a powerful approach toward understanding the molecular mechanisms of membrane assembly and membrane function. Application of such methods to the SR membrane were made possible by the initial efforts of Martonosi (40), who solubilized the $Ca^{2+}$ pump protein from SR with deoxycholate, and MacLennan (41), who achieved purification of this enzyme by fractionation with ammonium acetate. Various reconstitution procedures for SR have been developed by several investigators (10, 42–44) and efforts have

been extended to study the dominant factors in lipid-protein interactions (45). Martonosi (1) and Meissner and Fleischer (10, 19) pointed out the importance of removing membrane fragments not completely solubilized by deoxycholate and other detergents as a necessary prerequisite in developing a true reconstitution technique.

In this paper, we have characterized the activity of the RSR preparation originally developed by Meissner and Fleischer (19) and modified by Wang et al. (20) to prepare RSR over an extensive L/P range above and below the ratio normally observed in isolated SR. Their extensive work in methodology for defining conditions of the reconstitution technique has made possible the preparation of functional RSR vesicles over a wide range of L/P ratios. Most important, we have established that these membrane vesicles were capable of ATP-induced $Ca^{2+}$ uptake in the absence of $Ca^{2+}$ precipitating agents and with significant $Ca^{2+}$ uptake efficiency. In order to obtain the functional dependence of RSR on the L/P ratio we have measured estimates to the apparent initial rates and efficiencies of $Ca^{2+}$ uptake under conditions where the ATP concentration is submaximal for measuring the $Ca^{2+}$ uptake capacity. Therefore, when compared to isolated SR controls assayed under similar conditions, we are necessarily comparing the inherent efficiencies of the reconstituted and isolated SR membrane preparations. The *continuous* and *simultaneous* monitoring of the $Ca^{2+}$ uptake and ATPase kinetics of SR and RSR under nonsaturating conditions via the spectrophotometric approach (23) is thus both necessary and justifiable. Based on these considerations, we have reported here a RSR membrane system which is capable of transporting $Ca^{2+}$ with 80% of the velocity and with 35–45% of the efficiency of LSR controls, depending on the L/P ratio, as shown in Fig. 6, in the absence of $Ca^{2+}$ precipitating species. The $Ca^{2+}$ pumping efficiency may be much higher than this, as discussed below.

### *Some Characteristics of RSR Preparations*

HOMOGENEITY OF PREPARATIONS The extensive modifications in the methodology for preparing our RSR preparations has allowed an equally extensive characterization of the preparation with regard to its physical nature. The position on a sucrose gradient of RSR is critically dependent on its L/P ratio with smaller L/P preparations (i.e., greater protein content) banding at higher sucrose densities. These preparations are homogeneous with the statistical spread in the L/P molar ratio being on the order of $\pm$ 1%.

VESICULAR NATURE OF PREPARATIONS With the homogeneity of these preparations firmly established, several independent approaches have established the vesicular nature of RSR. Electron micrographs of solubilized SR before dialysis revealed the amorphous nature of the sample with no indication of the presence of fragmented membranes (data not shown, 20). After dialysis to remove detergent and purification of the preparation, each RSR preparation at a different L/P ratio clearly showed the formation of vesicles (Fig. 2). In addition, quasielastic light scattering measurements summarized in Table I on these dispersions revealed the presence of some polydispersity in vesicle size, the degree of polydispersity being similar for all RSR preparations and somewhat less than found for SR. Thus our RSR preparations are relatively homogeneous in size. Preliminary x-ray scattering data from RSR dispersions revealed that our RSR and SR preparations consist of unilamellar vesicles (see Paper II, Appendix A). Therefore, our RSR preparations are composed of unilamellar vesicles which are relatively homogeneous in density and size.

*Functional Dependence of RSR on L/P Ratio*

$Ca^{2+}$ ACCUMULATION LEVELS OF RSR The amount of $Ca^{2+}$ accumulated by RSR vesicles under submaximal conditions for measuring $Ca^{2+}$ uptake capacities, when normalized to equivalent intravesicular volumes (Fig. 5), is similar for each L/P ratio investigated. This implies that the $Ca^{2+}$ pump protein has not undergone any significant irreversible damage upon its dissociation and reconstitution with SR lipids to form membraneous vesicles. This is strengthened by the fact that when the $Ca^{2+}$ accumulation levels of LSR are likewise normalized with respect to the intravesicular volume of LSR, $Ca^{2+}$ accumulations of RSR using a limited supply of ATP are on the order of 85% that of LSR controls in a comparable time interval. These results thus represent a first measure of reconstitution of activity in our preparations.

INITIAL RATES OF $Ca^{2+}$ UPTAKE The investigation of the functional characteristics of the RSR system over the initial phase of the reaction with respect to LSR controls in the absence of oxalate is a fundamental one. A determination of the initial rates is necessary since (*a*) the initial rate of $Ca^{2+}$ transport would not be affected by differences in vesicle size; (*b*) the initial rates are independent of the leakiness of the vesicles; (*c*) the initial rates are independent of ATP and $Ca^{2+}$ concentrations as opposed to steady-state levels of accumulation (the concentrations of ATP and $Ca^{2+}$ utilized in our assays are well above their respective $K_m$ values); and (*d*) an analysis of the initial events of the reaction may allow a structure-function correlation for the RSR membrane when compared to isolated LSR. Thus we have calculated estimates to the initial rates of $Ca^{2+}$ uptake over the first 5 s of the reaction from kinetic traces similar to those shown in Fig. 4. The true initial rate, as determined over the first several hundred milliseconds of the reaction would not reflect the "leakiness" of the preparation. Though our determination of the apparent initial rate was calculated over the first 5 s interval, the "leak" term in the rate equation is minimal compared with its effect after several minutes of the reaction. In addition, the passive leak kinetics of RSR and LSR are very similar and we may temporarily ignore this constant factor in comparing their kinetics. Thus, even our estimated initial rates should then depend mainly upon the overall structural organization of the RSR membrane and may to some extent be affected by interactions of the protein and lipid components whose molar ratio we have manipulated especially at very low L/P ratios. The plot of the log of the initial uptake rates vs. the L/P ratios (Fig. 6*A*) reveals the functional capabilities of RSR as compared to LSR. The initial rates of $Ca^{2+}$ uptake by RSR with $L/P > 88$ have been shown to be 80% of the velocity of $Ca^{2+}$ transport observed for isolated LSR with a L/P ratio of 117. Owing to the variability of initial rate data obtained from membrane preparations, this result suggests but allows no distinction between two obvious models for the structural organization of these RSR membranes. First, the $Ca^{2+}$ pump protein molecules may be randomly (i.e., symmetrically) distributed in these RSR membranes with those pumps pointing in the proper direction possessing a greater efficiency to transport $Ca^{2+}$ as compared to LSR controls. Second 80% or more of the $Ca^{2+}$ pump protein may be unidirectionally oriented within the RSR membrane in a manner similar to that of isolated LSR, with these pumps having the same efficiency as in LSR. The asymmetric organization for these RSR membranes as suggested by electron microscopy (Fig. 2) and shown by a detailed structural analysis via x-ray and neutron diffraction techniques in the accompanying paper support the second alternative. However, the precise degree of unidirec-

tionality, which would distinguish between models I and II is presently unknown and cannot be inferred from the existing data. The initial rates of $Ca^{2+}$ uptake of RSR with L/P < 88 have between 30–60% of the velocity for transport compared to LSR (especially note that RSR with L/P between 50–60 have 30–40% of the velocity for $Ca^{2+}$ transport). This implies either a symmetrical distribution of the $Ca^{2+}$ pump protein for these RSR membranes (i.e., a significant portion of the $Ca^{2+}$ pumps point the wrong way) or an inactivation of a significant number of these pumps with the majority pointing the right way. The electron micrographs presented in this paper and in the accompanying paper would tend to support the former proposal. Nevertheless, these RSR membranes which function significantly poorer than LSR are structurally dissimilar when compared to either RSR (L/P > 88) or LSR (see paper II, Appendix A).

EFFICIENCY OF $Ca^{2+}$ UPTAKE The $Ca^{2+}$ uptake efficiency data summarized in Fig. 6*B* have a similar dependence on the L/P ratio, analogous to the initial rate data. Owing to the variability in the efficiencies of different preparations we obtain a family of curves of the same general shape, two of which appear in Fig. 6*B*. The lower curve represents one of our earlier preparations, characterized by atypically low efficiency values, but was included for the sake of completeness. Later preparations (top curve) typically revealed that RSR above approximately L/P ratio of 90 had efficiencies on the order of 35–45% that of LSR controls, whereas the efficiency values decreased dramatically for L/P < 80. However, this ratio calculated and shown in Fig. 6*B* represents the ratio of the initial $Ca^{2+}$ rate to the *total* ATPase rate in the absence of oxalate, as measured over the first 5 s, starting the reaction with the addition of ATP. Therefore, under these conditions, the $Ca^{2+}$-activated ATPase rate is equal to the total ATPase rate minus the basal ATPase rate.

In these RSR preparations, the basal ATPase rate (i.e., in the absence of added $Ca^{2+}$) may be significantly higher then that of isolated SR. We have measured the ratio of the $Ca^{2+}$ stimulated ATPase rate to the basal ATPase rate in isolated SR by the phenol red method and typically found it to be 15/1; for RSR with L/P > 88 the ratio was 3/1. These values were obtained under the conditions specified in this paper (i.e., reaction mixture composition, ATP, $Ca^{2+}$, and SR concentrations, pH etc.) and should not be directly compared with those obtained under dramatically different conditions (10, 19). Atomic absorption measurements of the endogenous $Ca^{2+}$ content in these experiments for isolated SR were on the order of 23 nmol/mg prot, and for RSR 10 nmol/mg prot. Hence, the ATPase rate in the absence of added $Ca^{2+}$ was measured in the presence of 50 and 500 $\mu$M EGTA in order to reduce the free $Ca^{2+}$ concentration levels to negligible amounts. Therefore, if the $Ca^{2+}$ uptake efficiency were expressed as the ratio of the initial $Ca^{2+}$ uptake rate to the $Ca^{+}$-stimulated ATPase rate in the absence of oxalate (i.e., subtracting the $Ca^{2+}$ independent ATPase rate from the total ATPase rate before calculating the efficiency), then the efficiencies in the absence of oxalate thus calculated would be much higher than they appear to be in Fig. 6*B*. Thus, we would find that for RSR with L/P > 88 all the preparations could have $Ca^{2+}$ uptake efficiencies > ~70% (i.e. ~0.4 nmol $Ca^{2+}$/nmol ATP) that of LSR (0.61 nmol $Ca^{2+}$/nmol ATP) comparable to the initial rate data shown in Fig. 6*A*.

*Functional Characteristics of RSR in the Presence of Oxalate*

The $Ca^{2+}$ loading rate and efficiency data presented in Fig. 7 have been included for the purpose of future reference. For the present time we offer neither an interpretation of these

data nor a mechanistic explanation of why it is different from the nonoxalate results. The differences in the results of these oxalate vs. nonoxalate assays may be due to the complex nature of the transport process under such dramatically different conditions, which is supported by the following previously published results: (*a*) Both the $Ca^{2+}$ stimulated and basal ATPase rates of SR are different in the presence or absence of oxalate, as shown by Inesi and Watanabe (46). (*b*) The relative concentrations of the reaction constituents in assays without oxalate (1 mg RSR/ml, 300 $\mu$M $Ca^{2+}$) are radically different. At the very least, the free $Ca^{2+}$ concentration relative to the SR concentration in the reaction medium is known to affect the ATPase activity of SR vesicles (47). (*c*) Oxalate permeability varies in different subcellular organelles, hence diffusion into reconstituted SR may be smaller than that in isolated LSR. (*d*) An additional variable is introduced in oxalate assays since the initial rates of oxalate-facilitated $Ca^{2+}$ uptake depend on both the $Ca^{2+}$ and oxalate concentrations (48).

Therefore, since it is not known what effects on the reaction mechanism of $Ca^{2+}$ transport may stem from these differences in the reaction mixtures of oxalate vs. nonoxalate assays, we feel there is at present no basis for a comparison of the two sets of results. Furthermore, since oxalate is a non-physiological constituent present in the reaction mixture, we feel that those assays carried out in the absence of oxalate are far more meaningful and we have used them in correlating the function and structure of the RSR membrane with LSR.

### *Conclusions*

We have shown that RSR membrane vesicles over an extended range of L/P ratios are capable of ATP-induced $Ca^{2+}$ uptake in the absence of $Ca^{2+}$ precipitating species, which reflects a true transport process. The estimates to the initial $Ca^{2+}$ uptake rates and efficiencies of RSR were found to be comparable to those of isolated LSR controls at comparable L/P ratios. These RSR membranes with L/P > 88 possess a structural asymmetry, as revealed by the heavy metal staining electron microscopic images of vesicular dispersions, which is similar to that observed for LSR. This is to be contrasted to RSR membranes at low L/P molar ratio (especially ~50–60), whose poor functional behavior may be related to a much different structural organization for these membranes as compared to both LSR and RSR at L/P ratios comparable to LSR (i.e. the distinctive symmetrical heavy-metal staining of vesicular dispersions of RSR at low L/P ratio). The precise degree of unidirectionality of the $Ca^{2+}$ pump protein in all RSR membranes, which we are currently pursuing, is presently unknown and cannot be inferred from the existing data. In this paper we emphasize only that our RSR preparations at L/P ratios comparable to LSR are functionally similar under certain conditions and probably more structurally relevant to LSR as suggested by the heavy metal staining electron microscope images of vesicular dispersions. In the accompanying paper, we fully address the structural organization of the RSR membrane via the combined x-ray and neutron diffraction approach.

The authors would like to thank Mrs. Christine Dettbarn and Mrs. Connie Tuvvy for their excellent technical assistance. We are indebted to Ms. Elaine Regan for preparation of the manuscript and to Ms. Barbara Bashford, Ms. Mary Jo Larsen, and Mr. Ken Ray for preparation of the figures.

This work was supported by grants from the National Institutes of Health HL 18708 to Drs. Blasie and Scarpa; AM 14632, Muscular Dystrophy Association of America to Dr. Wang and Fleischer; and by a Cell and Molecular Biology

Institutional Training Grant Fellowship to Dr. Herbette. Dr. Scarpa is an Established Investigator of the American Heart Association.

*Received for publication 22 October 1979 and in revised form 29 May 1981.*

## REFERENCES

1. Martonosi, A. 1971. Structure and function of sarcoplasmic reticulum membranes. *In* Biomembranes. L. A. Manson, editor. Plenum Press, New York. Vol. 1:191–256.
2. Inesi, G. 1972. Active transport of calcium ion in sarcoplasmic membranes. *Annu. Rev. Biophys. Bioeng.* 1:191–210.
3. Meissner, G., and S. Fleischer. 1974. Characterization, dissociation and reconstitution of sarcoplasmic reticulum. *In* Calcium Binding Proteins Elsevier Scientific Publishing Co., Amsterdam. 281–313.
4. MacLennan, D. H., and P. C. Holland. 1975. Calcium transport in sarcoplasmic reticulum. *Annu. Rev. Biophys. Bioeng.* 4:377–404.
5. Tada, M., T. Yamamoto, and Y. Tonomura. 1978. Molecular mechanism of active calcium transport by sarcoplasmic reticulum. *Physiol. Rev.* 58:1–79.
6. Porter, K., and G. E. Palade. 1957. Studies on the endoplasmic reticulum III. Its form and distribution in striated muscle cells. *J. Biophys. Biochem. Cytol.* 3:269–299.
7. Weber, A., A. Herz, and I. Reiss. 1963. On the mechanism of the relaxing effect of fragmented sarcoplasmic reticulum. *J. Gen. Physiol.* 46:679–702.
8. Martonosi, A., and R. Feretos. 1964. Sarcoplasmic reticulum I. The uptake of $Ca^{++}$ by sarcoplasmic reticulum fragments. *J. Biol. Chem.* 239:648–658.
9. Meissner, G., and S. Fleischer. 1971. Characterization of sarcoplasmic reticulum from skeletal muscle. *Biochim. Biophys. Acta.* 241:356–378.
10. Meissner, G., and S. Fleischer. 1973. $Ca^{2+}$ uptake in reconstituted sarcoplasmic reticulum vesicles. *Biochem. Biophys. Res. Commun.* 52:913–920.
11. Meissner, G. 1975. Isolation and characterization of two types of sarcoplasmic reticulum vesicles. *Biochim. Biophys. Acta.* 389:51–68.
12. MacLennan, D. H., P. Seeman, G. H. Isles, and C. C. Yip. 1971. Membrane formation by the adenosine triphosphatase of sarcoplasmic reticulum. *J. Biol. Chem.* 246:2702–2710.
13. McFarland, B. H., and G. Inesi. 1971. Solubilization of sarcoplasmic reticulum with Triton X-100. *Arch. Biochem. Biophys.* 145:456–464.
14. Rizzolo, L. J., M. LeMaire, J. A. Reynolds, and C. Tanford. 1976. Molecular weights and hydrophobicity of the polypeptide chain of sarcoplasmic reticulum calcium (II) adenosine triphosphatase and of its primary tryptic fragments. *Biochemistry.* 15:3433–3437.
15. DuPont, Y., S. C. Harrison, and W. Hasselback. 1973. Molecular Organization in the sarcoplasmic reticulum membrane studied by x-ray diffraction. *Nature. (Lond.).* 244:555–558.
16. Herbette, L., J. Marquardt, A. Scarpa, and J. K. Blasie. 1977. A direct analysis of lamellar x-ray diffraction from hydrated oriented multilayers of fully functional sarcoplasmic reticulum. *Biophys. J.* 20:245–272.
17. Herbette, L., C. T. Wang, A. Saito, S. Fleischer, A. Scarpa, and J. K. Blasie. 1981. A comparison of the profile structures of isolated and reconstituted sarcoplasmic reticulum membranes. *Biophys. J.* 36:47–72.
18. Worthington, C. R., and S. C. Liu. 1973. Structure of sarcoplasmic reticulum membranes at low resolution (17 Å). *Arch. Biochem. Biophys.* 157:573–579.
19. Meissner, G., and S. Fleischer. 1974. Dissociation and reconstitution of functional sarcoplasmic reticulum vesicles. *J. Biol. Chem.* 249:302–309.
20. Wang, C. T., A. Saito, and S. Fleischer. 1979. Correlation of ultrastructure of reconstituted SR membranes with changes in lipid and protein composition. *J. Biol. Chem.* 254:9209–9219.
21. Kamazawa, T., S. Yamada, T. Yamamoto, and Y. Tonomura. 1971. Reaction mechanism of the $Ca^{2+}$ dependent ATPase of sarcoplasmic reticulum from skeletal muscle. *J. Biochem. (Tokyo).* 70:95–123.
22. Meissner, G. 1973. ATP and $Ca^{2+}$ binding by the $Ca^{2+}$ pump protein of sarcoplasmic reticulum. *Biochim. Biophys. Acta.* 298:906–926.
23. Scarpa, A. 1978. Measurements of cation transport with metallochromic indicators. *Methods Enzymol.* 56:301–338.
24. Meissner, G., G. E. Conner, and S. Fleischer. 1973. Isolation of sarcoplasmic reticulum by zonal centrifugation and purification of $Ca^{2+}$ pump and $Ca^{2+}$ binding proteins. *Biochem. Biophys. Acta.* 298:246–269.
25. Lowry, O. H., N. J. Rosenbrough, A. L. Farr, and R. J. Randall. 1951. Protein measurement with folin reagent. *J. Biol. Chem.* 193:265–275.

26. Saito, A., C. T. Wang, and S. Fleischer. 1978. Membrane asymmetry and enhanced ultrastructural detail of sarcoplasmic reticulum revealed with use of tannic acid. *J. Cell Biol.* 79:601–616.
27. Scarpa, A., J. Baldassare, and G. Inesi. 1972. The effect of calcium ionophores on fragmented sarcoplasmic reticulum. *J. Gen. Physiol.* 60:735–749.
28. Alberty, R. A., R. M. Smith, and R. M. Bock. 1951. The apparent ionization constants of the adenosinephosphates and related compounds. *J. Biol. Chem.* 193:425–434.
29. Yamada, S., T. Yamamato, and Y. Tonomura. 1970. Reaction mechanism of the $Ca^{2+}$ -dependent ATPase of sarcoplasmic reticulum from skeletal muscle. *J. Biochem.* 67:789–794.
30. Fiske, C. H., and Y. Subbarow. 1925. The colorimetric determination of phosphorus. *J. Biol. Chem.* 66:375–400.
31. Chen, P. S., T. Y. Toribara, and H. Warner. 1956. Microdetermination of phosphorus. *Anal. Chem.* 28:1756–1758.
32. Johnson, R. G. and A. Scarpa. 1976. Ion permeability of isolated chromaffin granules. *J. Gen. Physiol.* 68:601–631.
33. O'Brien, R., and G. Brierley. 1965. Compartmentation of heart mitochondria I. Permeability characteristics of isolated beef heart mitochondria. *J. Biol. Chem.* 240:4527–4531.
34. Duggan, P. F., and A. Martonosi. 1970. Sarcoplasmic reticulum IX. The permeability of sarcoplasmic reticulum membranes. *J. Gen. Physiol.* 56:147–167.
35. Heldt, H. W., K. Werdan, M. Melancev, and G. Geller. 1973. Alkalization of the chloroplast stroma caused by light-dependent proton flux into the thylakoid space. *Biochim. Biophys. Acta.* 314:224–241.
36. Reijngoud, D. J., and J. M. Tager. 1973. Measurement of intralysosomal pH. *Biochim. Biophys. Acta.* 297:174–178.
37. Berne, B. J., and R. Pecora. 1976. Model systems of spherical molecules. *In* Dynamic Light Scattering with Applications to Chemistry, Biology, and Physics. Wiley & Sons, Inc., New York. 53–65.
38. Selser, J. C., Y. Yeh, and R. J. Baskin. 1976. A light-scattering characterization of membrane vesicles. *Biophys. J.* 16:337–346.
39. Inesi, G., and A. Scarpa. 1972. Fast kinetics of adenosine triphosphate-dependent $Ca^{2+}$ uptake by fragmented sarcoplasmic reticulum. *Biochemistry.* 11:356–359.
40. Martonosi, A. 1968. Sarcoplasmic Reticulum. IV. Solubilization of microsomal adenosine triphosphatase. *J. Biol. Chem.* 243:71–81.
41. MacLennan, D. H. 1970. Purification and properties of an adenosine triphosphatase from sarcoplasmic reticulum. *J. Biol. Chem.* 245:4508–4518.
42. Racker, E. 1972. Reconstitution of a calcium pump with phospholipids and a purified $Ca^{2+}$ adenosine triphosphatase from sarcoplasmic reticulum. *J. Biol. Chem.* 247:8198–8200.
43. Warren, G. B., P. A. Toon, N. J. M. Birdsall, A. G. Lee, and J. C. Metcalfe. 1974. Reconstitution of a calcium pump using defined membrane components. *Proc. Natl. Acad. Sci.* 71:622–626.
44. Repke, D. I., J. C. Spivak, and A. M. Katz. 1976. Reconstitution of an active calcium pump in sarcoplasmic reticulum. *J. Biol. Chem.* 251:3169–3175.
45. Moore, B. M., B. R. Lentz, and G. Meissner. 1978. Effects of sarcoplasmic reticulum $Ca^{2+}$-ATPase on phospholipid bilayer fluidity: boundary lipid. *Biochemistry.* 17:5248–5255.
46. Inesi, G., and S. Watanabe. 1967. Temperature dependence of ATP hydrolysis and calcium uptake by fragmented sarcoplasmic membranes. *Arch. Biochem. Biophys.* 121:665–671.
47. Carvalho, A. P., and U. M. C. Madeira. 1974. Biomembrane Lipids, Proteins, and Receptors, Burton and Packer, editors. Bi-Science, Webster Groves, Mo. 19:347–367.
48. Li, H. C., A. M. Katz, D. I. Repke, and A. Failor. 1974. Oxalate dependence of calcium uptake kinetics of rabbit skeletal muscle microsomes (fragmented sarcoplasmic reticulum). *Biochem. Biophys. Acta.* 367:385–389.